Σ^--nucleus interactions in emulsion at 350 GeV

M. Szarska, H. Wilczynski, W. Wolter, and K. Wozniak
Institute of Nuclear Physics, ul. Kawiory 26A, 30-055 Krakow, Poland

J. J. Lord and R. J. Wilkes
Department of Physics, FM-15, University of Washington, Seattle, Washington 98195
(Received 25 August 1992)

Experimental data on multiplicities and angular distributions of heavy ionizing and shower particles in inelastic interactions of 350 GeV Σ^- hyperons in nuclear emulsion are presented. The data are compared with the results of other experiments on proton and pion interactions in emulsion at energies of 60–800 GeV. We observe no significant differences in the global characteristics of strange hyperon interactions relative to nonstrange baryon interactions at equivalent energies, other than those attributable to the differing cross sections.

PACS number(s): 13.85.Hd, 13.85.Ni, 14.20.Jn

I. INTRODUCTION

Hyperon beams became available in the late 70's and provided a tool for the study of hyperon properties and baryon structure (for reviews see [1–3]). However, experimental data on multiparticle production in hyperon interactions has been very scarce. Here we present results on Σ^--emulsion interactions at 350 GeV, including the general characteristics of inelastic interactions of Σ^- with emulsion nuclei, and the multiplicity and angular distributions of produced relativistic charged particles as well as particles which are the products of disintegration of the target nucleus. Nuclear emulsion is well suited to study hadron-nucleus interactions thanks to its essentially 100 percent efficiency for detection of produced particles and the possibility of simultaneous observation of produced particles and those from the fragmentation of the target nucleus. This allows us to study multiparticle production as a function of the number of intranuclear collisions ν, estimated from the magnitude of the target nucleus excitation.

To see whether the presence of a strange quark in Σ^- somehow affects the process of multiparticle production we compared the results obtained from the analysis of Σ^--emulsion interactions with those from proton-emulsion and pion-emulsion experiments [4–16]. It is well known that both proton and pion interactions with nuclei are well described by the incoherent superposition of multiple nucleon-nucleon collisions [17–19]. In this approach the inelastic cross section $\sigma_{\rm inel}$ plays an essential role for the projectile-nucleon collision. The value of $\sigma_{\rm inel}$ is different for Σ^-, π^-, and p collisions and in the hundred GeV energy range was taken as 32.5 [20] and 20.7 mb [21] for pN and π^-N, respectively. Using the value of the total cross section measured at 137 GeV [2], we estimated the inelastic cross section for Σ^-N at 350 GeV to be 28 mb. Our analysis has shown that Σ^-, like π^- and p interactions with nuclei, are satisfactorily described by superposition models, and that the observed differences in some parameters describing the interactions of Σ^-, π^-, and p interactions with nuclei can be attributed to the different cross sections of the projectile on nucleons.

II. EXPERIMENTAL DATA

In our experiment (E730 at Fermi National Accelerator Laboratory) we exposed stacks composed of Fuji ET7B and Ilford G5 nuclear emulsion pellicles (200 μm or 400 μm thick) to the 350 GeV/c hyperon beam. The primary 400 GeV/c proton beam was incident on a copper target and the secondary beam was defined by a curved channel in a tungsten plug placed in the Hyperon Targeting Magnet (for details see [22]). The emulsion stacks were placed 87 cm downstream from the magnet. In the setup used in our experiment, only secondary particles of negative charge produced at $p_t \simeq 0$ with momentum $p \simeq 350$ GeV/c could traverse the channel. Using the production ratios $N(\Sigma^-)/N(\pi^-)$ and $N(\Xi^-)/N(\Sigma^-)$ given in [22] we can estimate the secondary beam composition produced at the target as 96.3% , 3.2%, and 0.5% for Σ^-,π^-, and Ξ^-, respectively. The production of other possible secondaries was negligible and was not taken into further account in our calculations. Also, in the following analysis Ξ^- hyperons were treated as Σ^-. Due to the decays, $\Sigma^- \rightarrow n\pi^-$, the beam composition changed with distance from the target. However, pions from the decays of Σ^- had momenta between 13.2 and 126 GeV/c and due to their bending in the magnetic field, the majority were absorbed in the channel walls. Only those from decays which occurred close to the end of the channel or between the magnet and the emulsion stack had a chance to reach the emulsion. In order to find nuclear interactions in emulsion we used along-the-track scanning, in which we followed only those tracks for which the divergence angle with respect to the beam direction was less than 1 mrad. Since the decay angles of pions were in most cases greater than the scanning rejection angle, almost all pions from decays (except some with momenta close to 126 GeV/c or 13.2 GeV/c, i.e., emitted forward and backward in the rest frame of a Σ^-), were rejected

from the scanning. Using 286 mb for the inelastic cross section of π^--emulsion interactions and 339 mb for Σ^--emulsion we calculated the composition of our sample of 548 inelastic interactions in emulsion, as shown in Table I.

The mean free path for inelastic Σ^--emulsion interactions was found to be $\lambda = 38.4 \pm 1.5$ cm, which corresponds to a cross section of 330 ± 13 mb. The quantities measured in our experiment were corrected for the admixture of pion interactions. However these corrections were always much smaller than the statistical errors, and never exceed about 0.3% .

For comparison with Σ^--emulsion interactions we used data on π^--emulsion interactions at 60 GeV [4], 200 GeV [4], and 300 GeV [6, 7] as well as proton-emulsion interactions at 67 GeV [4], 200 GeV [8–11], 400 GeV [12], and 800 GeV [13–16] GeV. Altogether we used 3876 and 6380 pion and proton interactions, respectively. The scanning and measurement of σ, pion, and proton interactions in emulsion were carried out using the same experimental criteria.

Tracks associated with the interaction were classified according to their ionization employing the standard terminology used in nuclear-emulsion techniques. In each event we define the following multiplicity categories: n_s—shower particles ($\beta \geq 0.7$), tracks with ionization $I \leq 1.4I_0$, where I_0 denotes the minimum ionization produced by fast singly charged particles; N_g and N_b—grey and black tracks, which are often combined as $N_h = (N_b + N_g)$—heavy tracks. These tracks are formed by slow ($\beta < 0.7$) heavily ionizing, $I > 1.4I_0$, particles emitted from the target nucleus. The black tracks are produced by low-energy single and multicharged fragments emitted from the excited target nucleus while the grey tracks are due mainly to recoil protons. The latter have ionization less than about eight times minimum, which corresponds to the ionization of a ~ 30 MeV proton. The polar (θ) and azimuthal (ϕ) emission angles of all the tracks emitted from each inelastic Σ^--emulsion interactions were measured.

III. EXPERIMENTAL RESULTS

A. Heavily ionizing particles

In Figs. 1 and 2 we present the multiplicity distributions of grey and black tracks for interactions of Σ^-, π^-, and p in nuclear emulsion. Taking into account the well-known independence [6, 13, 23] of the multiplicity distributions of heavy ionizing particles on energy of the projectile we plotted in Figs. 1 and 2 the compound distributions for 60, 200, and 300 GeV π^- emulsion, and 67, 200, 400, and 800 GeV p-emulsion interactions. The corresponding mean values are given in Table II.

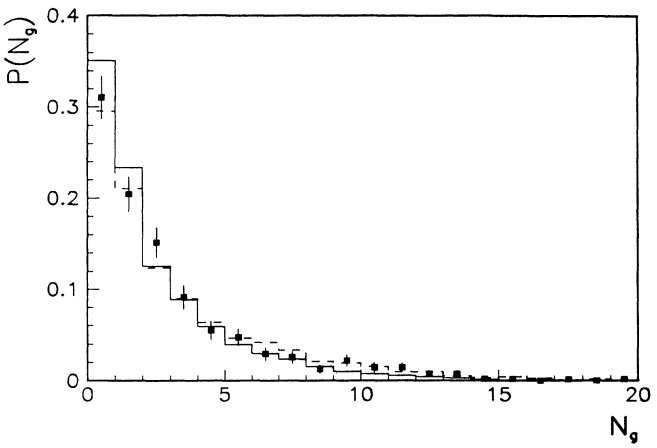

FIG. 1. The multiplicity distributions of grey tracks N_g for Σ^- (data points), π^- (solid line), and p (dashed line), interactions in emulsion.

The difference between the mean values $\langle N_g \rangle$ of grey tracks for π^- and Σ^- interactions with emulsion is evident. The fact that the multiplicity distribution of grey tracks is similar to that for p-emulsion interactions is illustrated in Fig. 3 where the integral distributions of grey tracks are plotted.

The angular distributions of grey tracks for Σ^-, π^-, and p interactions, normalized to the same area, are presented in Fig. 4. One can see that the shapes of the angular distributions are the same for the three projectiles considered.

Taking into account all the experimental data presented above one can conclude the following: (a) the mechanism of slow particle production is the same for Σ^-, π^-, and p interactions with nuclei, (b) the shape of the angular distribution of grey tracks, namely its strong anisotropy, indicates that these tracks are mainly due to recoil protons, and (c) the observed differences in the multiplicity distributions and their mean values can be explained by different cross sections of Σ^-, π^-, and p on nucleons. This will be illustrated in the next section.

TABLE I. Statistical composition of the event sample, estimated as described in the text.

Projectile	Percentage	
Σ^--Em (350 GeV/c)	94.8%	+ 1.4% −2.0%
π^--Em (350 GeV/c)	5.0%	+ 2.0% −1.4%
π^--Em (126 GeV/c)	0.2%	
π^--Em (13.2 GeV/c)	0.002%	

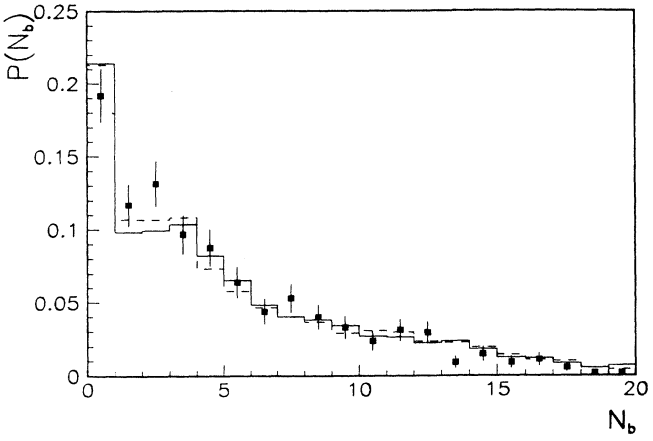

FIG. 2. The multiplicity distributions of black tracks N_b for Σ^- (data points), π^- (solid line), and p (dashed line), interactions in emulsion.

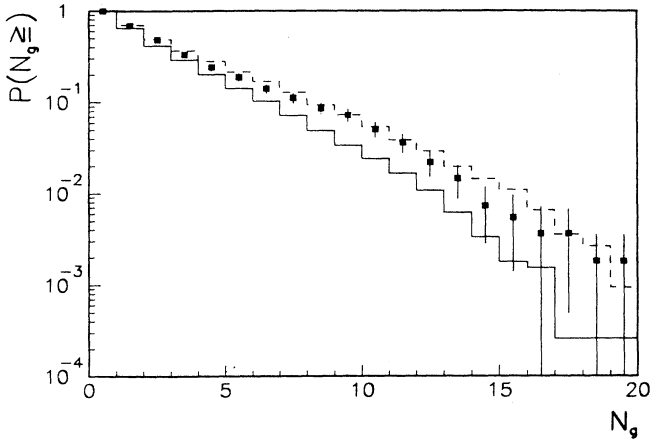

FIG. 3. The integral multiplicity distributions of grey tracks N_g for Σ^- (points), π^- (solid line), and p (dashed line), interactions in emulsion.

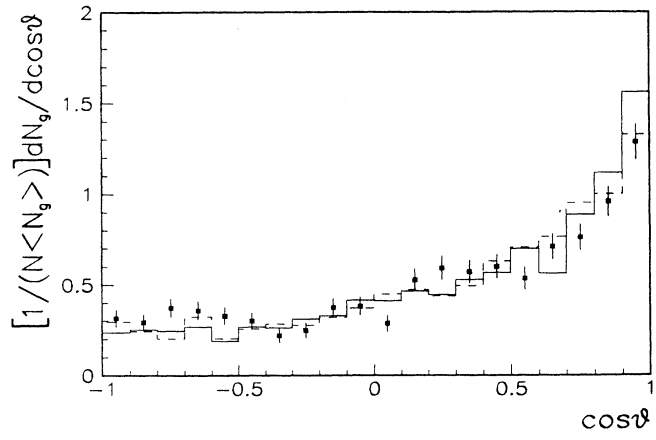

FIG. 4. The angular distributions of grey tracks N_g normalized to the same area for Σ^- (data points), π^- (solid line), and p (dashed line), interactions in emulsion.

B. Relativistic particles

The distribution of the multiplicity of shower particles n_s produced in Σ^--emulsion interactions is depicted in Fig. 5 and its mean value and dispersion are 15.22 ± 0.42 and 9.38 ± 0.36, respectively. One can see that the highest multiplicity encountered does not exceed about 55 charged particles. In Fig. 6 we present the multiplicity distributions of produced particles in Σ^-, π^-, and p interactions in emulsion using the Koba-Nielsen-Olesen (KNO) [24] scaling variable. One can see that the distribution for Σ^- interactions does not differ within the statistical errors from those for π^- and protons. In Fig. 7 we show the mean multiplicity $\langle n_s \rangle$ of shower particles for interactions of pions, protons and Σ^- as a function of the projectile-proton c.m. energy squared. The proton and pion data are well fitted by straight lines with different coefficients and the mean multiplicity of produced particles for Σ^- interactions lies between these lines. This is in accordance with expectation due to the different cross sections of Σ^-, π^-, and p interactions with nucleons.

In Fig. 8 is shown the inclusive angular distribution in pseudorapidity [$\eta = -\ln\tan(\theta/2)$] of shower particles n_s produced in Σ^--emulsion interactions. Unfortunately direct comparison of the pseudorapidity distribution of produced particles for Σ^- interactions with those for pion and proton interactions is impossible due to the lack of pion and proton data at 350 GeV. The only possibility is to use some parameters describing the pseudorapidity distribution of produced particles in Σ^--emulsion interactions at 350 GeV with the energy dependence of these parameters for pion and proton interactions. We have applied this procedure to compare the following parameters: the mean value $\langle \eta \rangle$ (Fig. 9), the dispersion D of the distribution (Fig. 10) and the pseudorapidity density ρ_c in the central region (Fig. 11) calculated in a window of the width 1.6 centered at $\langle \eta \rangle$. We would like to point out two features which follow from these comparisons. The first one is a linear dependence of $\langle \eta \rangle$, D, and ρ_c on s, the second one concerns the magnitudes of the examined parameters for Σ^--emulsion interactions. The value of $\langle \eta \rangle$ and D for Σ^- emulsion is consistent with

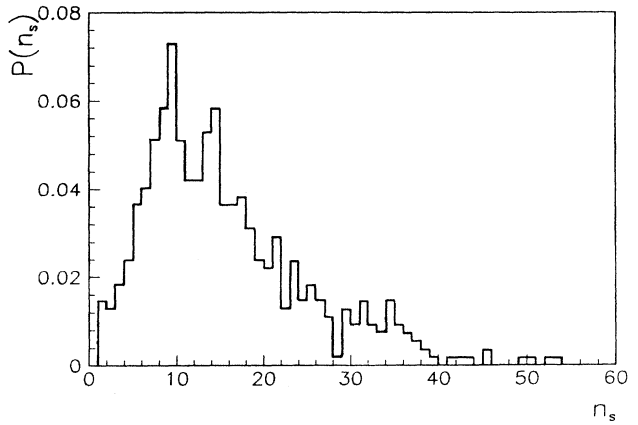

FIG. 5. The multiplicity distribution of shower particles n_s for Σ^- interactions in emulsion.

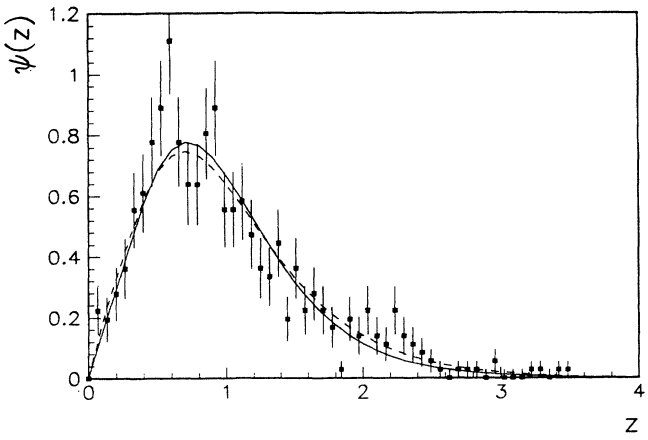

FIG. 6. The KNO scaling function $[\psi(z) = \langle n_s \rangle P(n_s)$, where $z = n_s/\langle n_s \rangle]$ for Σ^- interactions in emulsion (data points). Fits for π^- (solid line) [6], and for p (dashed line) [13], are also shown.

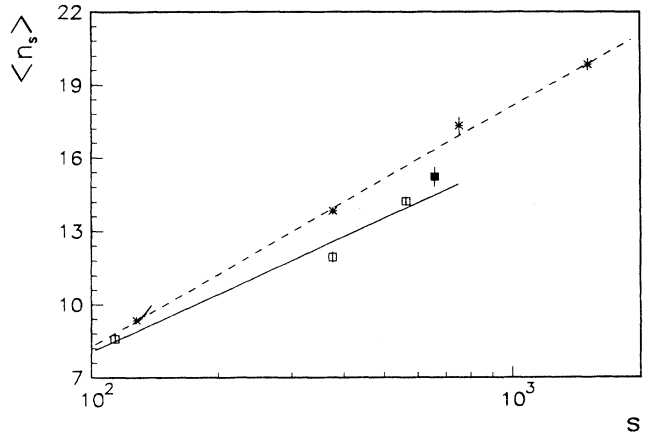

FIG. 7. The mean multiplicity of shower particles $\langle n_s \rangle$ for Σ^- (filled squares), π^- (open squares), and p (crosses), interactions in emulsion as a function of proton-proton c.m. energy squared s [GeV^2]. Lines are the best fit to the pion and proton experimental data.

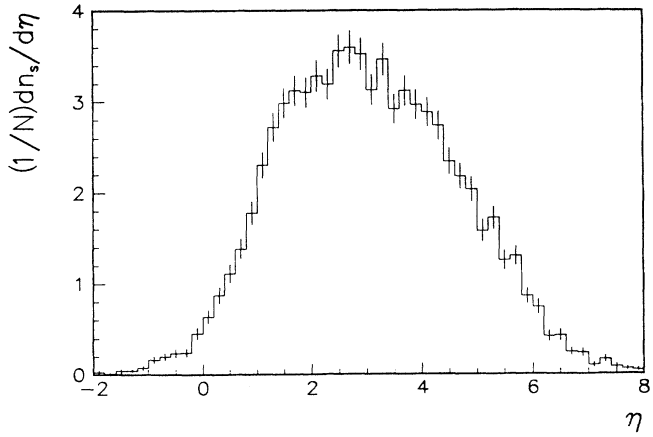

FIG. 8. The pseudorapidity distribution of relativistic particles (n_s) for Σ^- interactions in emulsion.

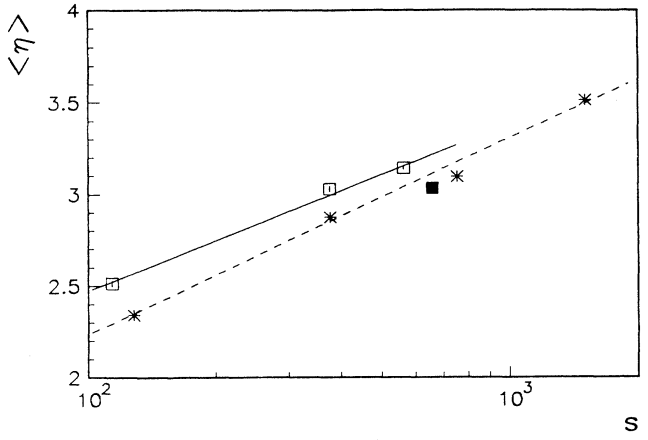

FIG. 9. The dependence of the mean value $\langle \eta \rangle$ of pseudorapidity distributions of shower particles n_s on the proton-proton c.m. energy squared s [GeV^2] for Σ^- (filled squares), π^- (open squares), and p (crosses), interactions in emulsion. Lines are the best fit to the pion and proton experimental data.

that for proton-emulsion interaction and the ρ_c for Σ^- is in between the values for proton and pion data. This is evidence that multiparticle production is controlled by the magnitude of the cross section of the projectile-nucleon collision. This behavior is a consequence of the superposition of intranuclear hadron-nucleon collisions in hadron-nucleus interactions. We will now see whether the superposition model describes Σ^--nucleus interaction as well as it does π^- [23, 29] and proton-nucleus interactions [15, 16, 23]. To do this we use grey tracks as a measure of the number ν of intranuclear projectile-nucleon collisions. This is a widely used method [17–19, 25–28] in nuclear-emulsion experiments which allows us to divide the inclusive sample of interactions into sub-

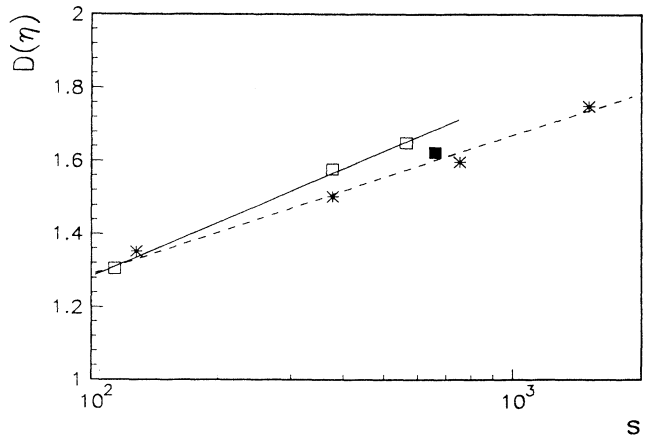

FIG. 10. The dependence of the dispersion D of pseudorapidity distributions of shower particles n_s on the proton-proton c.m. energy squared s [GeV^2] for Σ^- (filled squares), π^- (open squares), and p (crosses), interactions in emulsion. Lines are the best fit to the pion and proton experimental data.

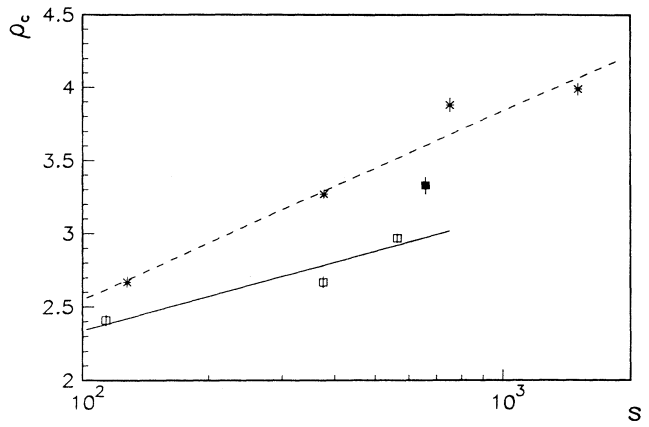

FIG. 11. The dependence of the pseudorapidity density ρ_c in the central region of shower particles n_s on the proton-proton c.m. energy squared s [GeV^2] for Σ^- (filled squares), π^- (open squares), and p (crosses), interactions in emulsion. Lines are the best fit to the pion and proton experimental data.

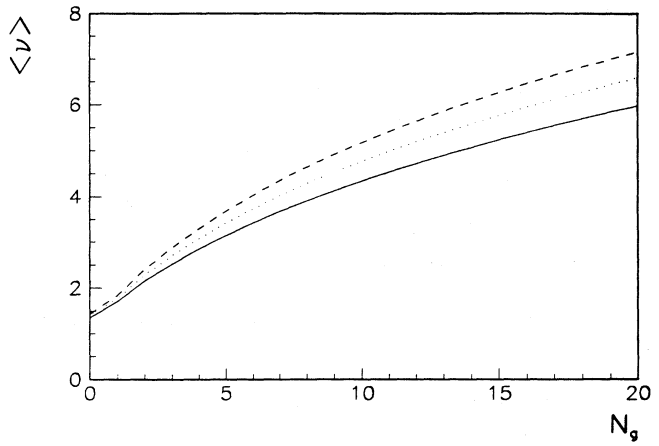

FIG. 12. The dependence of the mean number $\bar{\nu}$ of intranuclear nucleon-nucleon collisions on the number N_g of grey tracks for Σ^- (dotted line), π^- (solid line), and p (dashed line), interactions in emulsion.

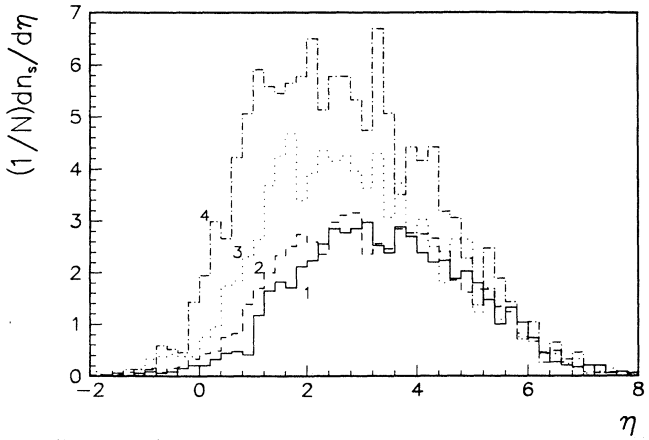

FIG. 13. The pseudorapidity distributions of shower particles n_s for groups of Σ^- interactions in emulsion with different mean values $\bar{\nu}$ of intranuclear nucleon-nucleon collisions. Histograms 1 to 4 correspond to $\bar{\nu}$=1.39, 2.00, 2.98, and 4.47, respectively. For details see Table III.

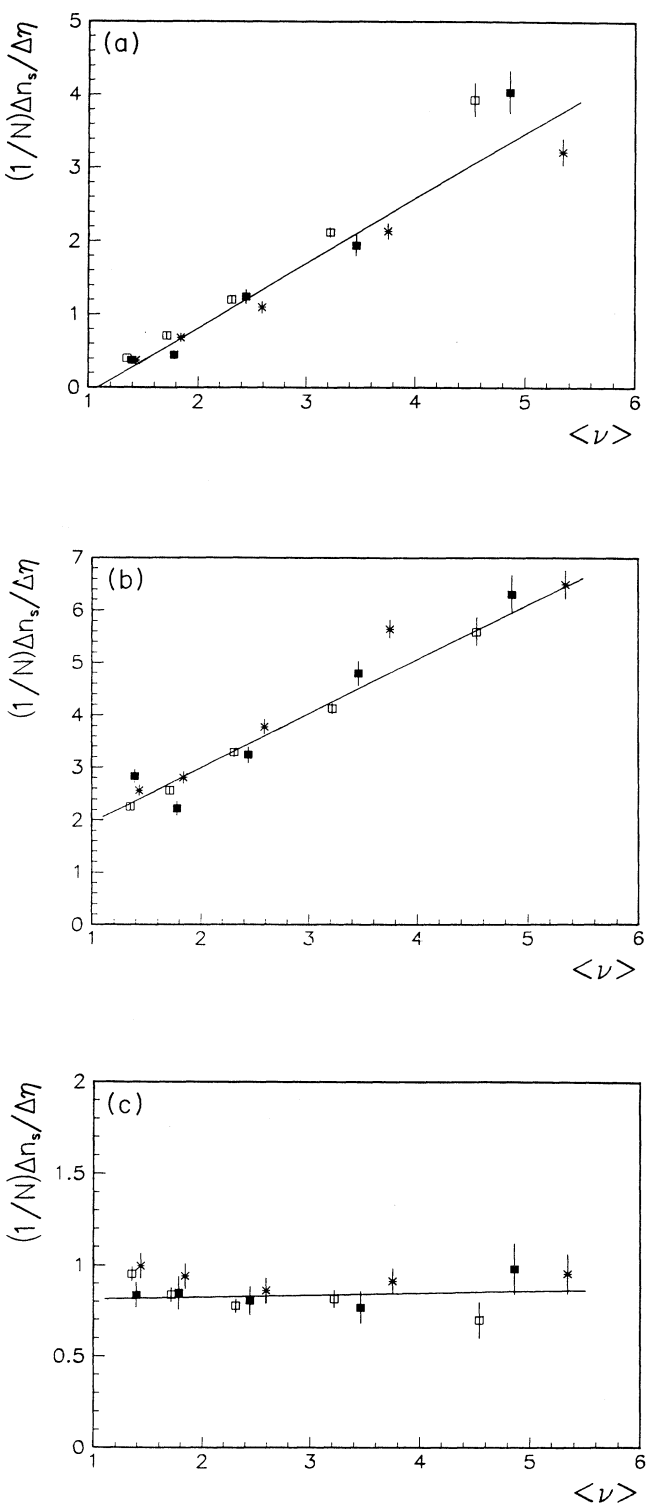

FIG. 14. The pseudorapidity density integrated over the pseudorapidity intervals: (a) $0 \leq \eta \leq 1$, (b) $2.5 \leq \eta \leq 3.5$, (c) $5.5 \leq \eta \leq 6.5$ as a function of the mean number $\bar{\nu}$ of intranuclear nucleon-nucleon collisions for 350 GeV Σ^- (solid squares), 300 GeV π^- (open squares), and 400 GeV p (crosses), interactions in emulsion. The line was fitted to Σ^- data only.

TABLE II. Average multiplicities of heavy ionizing particles.

Projectile	E_0 (GeV)	N_{ev}	$\langle N_g \rangle$	$\langle N_b \rangle$
π^-	60–300	3876	2.02±0.04	4.92±0.08
Σ^-	350	548	2.53±0.14	4.40±0.21
p	67–800	6380	2.73±0.04	4.80±0.06

samples with different values of $\bar{\nu}$. Without going into details of the applied method (see, e.g., [17]) we present in Fig. 12 the relation between the mean number $\bar{\nu}$ of intranuclear collisions, and the number N_g of grey tracks in Σ^--emulsion interactions. For comparison we also plotted the same relation for π^- and p-emulsion interactions. The curves plotted in Fig. 12 are different because the corresponding cross sections are different, i.e., $\sigma(\pi^- N) < \sigma(\Sigma^- N) < \sigma(pN)$. Thus for a fixed number N_g one obtains $\bar{\nu}(\pi^- - \mathrm{Em}) < \bar{\nu}(\Sigma^- - \mathrm{Em}) < \bar{\nu}(p - \mathrm{Em})$.

We divided the inclusive sample of Σ^--emulsion interactions into four subsamples characterized by different numbers N_g of grey tracks. The corresponding values of $\bar{\nu}$ were calculated from the relation $\bar{\nu}$ vs N_g shown in Fig. 12. The number N of events in each interval of N_g tracks the corresponding number $\bar{\nu}$ of intranuclear collisions and the mean number $\langle n_s \rangle$ of produced particles are given in Table III together with the mean value $\langle \eta \rangle$ of pseudorapidity distribution and its dispersion $D(\eta)$.

In Fig. 13 we plot the pseudorapidity distributions of produced particles n_s for interactions with different values of $\bar{\nu}$. One can see that with increasing $\bar{\nu}$ the multiplicity of produced particles increases and the pseudorapidity distribution shifts toward lower values of η while the dispersion of the distribution remains unchanged (see Table III).

In order to analyze in more detail the dependence of pseudorapidity distributions of produced particles on the number ν of intranuclear collisions, we investigated the density $\rho(\eta)$ of produced particles as a function of ν in three distinct intervals of pseudorapidity, namely: the target fragmentation region $0 \leq \eta < 1$, the central region $2.5 \leq \eta < 3.5$, and the projectile fragmentation region $5.5 \leq \eta < 6.5$. In Fig. 14 the results for Σ^--emulsion interactions are shown and compared to those for 300 GeV π^--emulsion and 400 GeV p-emulsion interactions. Direct comparison between these data is not possible because of different projectile energies and different kinematics (especially in the projectile fragmentation region), but we can see very similar general trends. The dependence $\rho(\eta)$ on $\bar{\nu}$ can be approximated by a linear relation. The increase of density $\rho(\eta)$ as indicated by the slope is similar in the target fragmentation and central region while for the projectile fragmentation region the density becomes nearly constant.

IV. SUMMARY AND CONCLUSIONS

In this paper we have presented the experimental data on 548 inclusive Σ^--emulsion interactions at 350 GeV. We have investigated multiplicity and angular distributions of both the heavy ionizing particles (target fragments) and the relativistic particles produced in interactions. Results were compared with those of proton and pion interactions in emulsion. We do not observe any qualitative differences in the global characteristics of inelastic interactions of the strange baryon Σ^- from those observed in pion and proton interactions. Some quantitative differences in parameters describing the interactions can easily be explained by the different cross-sections for pion, σ hyperon, and proton on nucleons. These differences refer to such quantities as multiplicity and angular distributions both of the produced particles and of those emitted from the struck target nucleus. The general features of Σ^- interactions, like pion and proton interactions, are consistent with the assumption of incoherent superposition of intranuclear projectile-nucleon collisions.

ACKNOWLEDGMENTS

We would like to express our thanks to Professor J. Lach, to Dr. S. Krzywdzinski, and to the staff of Fermi National Accelerator Laboratory for their great help in the preparation of the experiment and during the 350 GeV Σ^- exposure. We also wish to thank Professor R. Hołynski for valuable and stimulating discussions and for critical reading of this manuscript.

TABLE III. Parameters describing pseudorapidity distributions of produced particles in Σ^--Em collisions with different degrees of centrality.

N_g	N_{ev}	$\bar{\nu}$	$\langle n_s \rangle$	$\langle \eta \rangle$	$D(\eta)$
0	170	1.39	11.55±0.47	3.39±0.04	1.56±0.02
1–2	195	2.00	12.79±0.52	3.20±0.03	1.61±0.02
3–5	106	2.98	17.52±0.96	2.85±0.04	1.60±0.03
>5	77	4.47	25.94±1.18	2.65±0.04	1.61±0.02

[1] J. Lach and L. Pondrom, Annu. Rev. Nucl. Sci. **29**, 203 (1979).
[2] M. Bourguin and J. P. Repellin, Phys. Rep. **114**, 100 (1984).
[3] J. Lach, Report No. Fermilab-Conf-91/200, 1991 (unpublished).
[4] J. Babecki *et al.*, Acta Phys. Pol. B **9**, 495 (1978).
[5] Z. V. Anzon *et al.*, Nucl. Phys. **B129**, 205 (1977).
[6] J. Babecki *et al.*, Acta Phys. Pol. B **16**, 323 (1985).
[7] R. Holynski *et al.*, Acta Phys. Pol. B **17**, 201 (1986).
[8] J. Babecki *et al.*, Phys. Lett. 47B, **268** (1973).
[9] J. Babecki *et al.*, Acta Phys. Pol. B **5**, 315 (1974).
[10] Alma Ata-Leningrad-Moscow-Tashkent Collaboration, E. V. Anzon *et al.*, Yad. Fiz. **22**, 736 (1975) [Sov. J. Nucl. Phys. **22**, 380 (1975)].
[11] S. A. Azimow *et al.*, Yad. Fiz. **26**, 346 (1977) [Sov. J. Nucl. Phys. **26**, 180 (1977)].
[12] I. Otterlund (private comunication).
[13] A. Abduzhamilov *et al.*, Phys. Rev. D **35**, 3537 (1987).
[14] A. Abduzhamilov *et al.*, Z. Phys. C **40**, 223 (1988).
[15] A. Abduzhamilov *et al.*, Z. Phys. C **40**, 1 (1988).
[16] A. Abduzhamilov *et al.*, Phys. Rev. D **39**, 86 (1989).
[17] J. B. Andersson *et al.*, Phys. Lett. **73B**, 343 (1978).
[18] M. K. Hegab and J. Hufner, Phys. Lett. **105B**, 103 (1981).
[19] M. K. Hegab and J. Hufner, Nucl. Phys. **A384**, 353 (1982).
[20] High Energy Reaction Analysis Group, V. Flamino *et al.*, CERN-HERA Report No. 84-01 1984 (unpublished).
[21] V. Flamino *et al.*, "Compilation of Cross-Sections: π^+ and π^- Induced Reactions," CERN-HERA Report No. 83-01, 1983 (unpublished).
[22] T. R. Cardello *et al.*, Phys. Rev. D **32**, 1 (1985).
[23] R. Holynski, IFJ - Report No. 1303/PH, Krakow, 1986 (unpublished).
[24] Z. Koba, H. B. Nielsen, and P. Olesen, Nucl. Phys. **B40**, 317 (1972).
[25] B. Furmanska *et al.*, Acta Phys. Pol. B **8**, 973 (1977).
[26] J. Babecki and G. Nowak, Acta Phys. Pol. B **9**, 401 (1978).
[27] A. Jurak, IFJ - Report No. 988/PH, Krakow, 1977 (unpublished).
[28] E. Stenlund and I. Otterlund, Nucl. Phys. **B198**, 407 (1982).
[29] R. Holynski *et al.*, Z. Phys. C **31**, 467 (1986).